Kan Song*, Jun Zhang and Lin Liu

Hypereutectic Al_2O_3/YAG/ZrO_2 In Situ Composite Prepared by Horizontal Laser Zone Melting

DOI 10.1515/htmp-2015-0147
Received July 1, 2015; accepted November 24, 2015

Abstract: Al_2O_3/YAG/ZrO_2 eutectic in situ composite has now been considered as the new generation of high-temperature structural material due to its excellent performance even close to its melting point. In this work, hypereutectic Al_2O_3/YAG/ZrO_2 in situ composite is manufactured by the horizontal laser zone melting technique. The relationship between the solidification microstructure and the solidification parameters is studied. The minimum lamellar spacing is as finer as 0.20 μm when the laser scanning rate is 800 μm/s. Compared with eutectic Al_2O_3/YAG/ZrO_2, hypereutectic exhibits more regular and finer microstructure at the similar conditions. Meanwhile, it is found that the lamellar spacing remains almost as constant at a certain high solidification velocity. The maximum hardness and fracture toughness are 15.9 GPa and 4.2 MPa · $m^{1/2}$, respectively.

Keywords: Al_2O_3/YAG/ZrO_2, hypereutectic, horizontal laser zone melting

Introduction

In 1997, Waku [1] found Al_2O_3/YAG binary eutectic in situ composite that possesses outstanding mechanical properties and chemical stabilities at high temperature. The flexural strength at 2,073 K is 360–500 MPa [2]. The compression creep strengths [3] at 1,873 K is about 433 MPa under the strain rate of 10^4/s. However, recent research indicates that Al_2O_3/YAG eutectic in situ composite does not have optimistic corrosion resistance under the conditions simulating the aeroengine working environment [4]. During corrosion exposure under high-velocity and high-temperature gas flow of water vapor, water vapor led to the favored degradation of the alumina phase. Aluminates like YAG, YAP and YAM show a superior corrosion resistance in comparison to alumina, and more than one order in magnitude lower corrosion rate [5]. Therefore, the sample showed the formation of porous YAG surface due to gasification of alumina, and then, the porous layer crack and spall. For the longtime exposure of Al_2O_3/YAG eutectic in situ composite in gas turbines, the use of environmental barrier coatings like dense YAG is proposed. But in the view of solidification scholars, that is not the exclusive way. For instance, refinement of lamellar spacing (prevent penetration of corrosion flow into the layer), the decrease of alumina content, all of the above are possible methods to enhance the corrosion resistance.

The lower toughness (≈2 Mpa · $m^{1/2}$) [6] is another bottleneck restricting the application of Al_2O_3/YAG eutectic in situ composite. The introduction of ZrO_2 into the eutectic composition is a widely used approach, enhancing the fracture toughness. In 2001, Lee [7] obtained Al_2O_3/YAG/ZrO_2 ternary eutectic fibers 0.3–2 mm in diameter and 500 mm in length grown with the micro-pulling-down (μ-PD) method. Compared with Al_2O_3/YAG eutectic obtained under similar solidification condition [8], Al_2O_3/YAG/ZrO_2 eutectic exhibits finer microstructure and higher fracture toughness due to the addition of the third component and the strengthening effect of ZrO_2 [9, 10]. From that, Al_2O_3/YAG/ZrO_2 ternary with eutectic composition was widely investigated [11–13]. With the increase of solidification velocity, microstructure morphology is finer and more regular. The microstructure transforms from the so-called Chinese script to texturing morphology; therefore, the mechanical properties exhibit more anisotropy. The fracture toughness of Al_2O_3/YAG/ZrO_2 eutectic in situ composite prepared by the laser floating zone is 4.3 Mpa · $m^{1/2}$, as higher as twice of that obtained from Al_2O_3/YAG eutectic [14].

Furthermore, almost all works were concentrated on the eutectic point that with off-eutectic composition was seldom concerned. But for revealing the solidification behavior of Al_2O_3/YAG/ZrO_2 ternary system, the investigations with off-eutectic composition are indispensable. Otherwise, from the thermodynamic point of view, the full lamellar microstructure can also be obtained with off-eutectic composition under nonequilibrium solidification condition.

***Corresponding author: Kan Song,** State Key Laboratory of Solidification Processing, Northwestern Polytechnical University, Xi'an 710072, P. R. China; School of Power and Energy, Northwestern Polytechnical University, Xi'an 710072, P. R. China, E-mail: songkan863@mail.nwpu.edu.cn
Jun Zhang, Lin Liu, State Key Laboratory of Solidification Processing, Northwestern Polytechnical University, Xi'an 710072, P. R. China

In conclusion, with the composition range in which the full lamellar microstructure can be obtained, seeking the suitable composition with less Al_2O_3 content and technology parameters, to obtain defect-free Al_2O_3/YAG/ZrO_2 ternary in situ composite with texturing morphology, are main development directions of this system. Considering the contribution of ZrO_2 to microstructure refinement and toughness enhancement, in this paper, the selected mole ratio of hypereutectic composition was Al_2O_3/YAG/ZrO_2 = 64.6:15.3:20.1, in which the ratio of Al_2O_3/YAG equaled to the ternary eutectic point, the ZrO_2 content, was added to 1.5 %.

Experimental

Ceramics were manufactured using a mixture of powders of Al_2O_3 (4 N), Y_2O_3 (4 N) and ZrO_2 (3 N) (64.6 mol% Al_2O_3, 15.3 mol% Y_2O_3, 20.1 mol% ZrO_2). The preparation of the precursor is described in detail elsewhere [15]. The experimental setup of the laser horizontal zone melting is schematically shown in Figure 1. The precursors were moved by the numerically controlled worktable to achieve the laser scanning with different velocities. The experiments were conducted under the Ar atmosphere with a laser power of about 200 W, a scanning rate of 100–800 μm/s and a beam diameter of 4 mm.

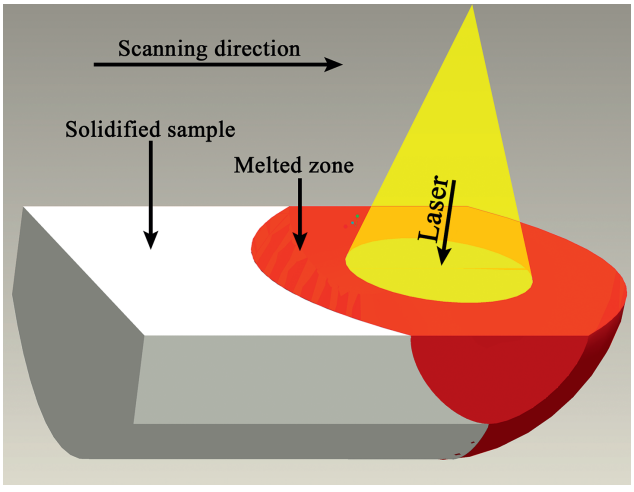

Figure 1: Schematic diagram of the laser horizontal zone melting.

The solidified samples were ground with SiC abrasive paper and polished sequentially with diamond paste down to 0.5 μm size. The sample surfaces were coated with a thin layer of Au before observation. The microstructure and component were examined by scanning electron microscopy (SEM) (JSM-5800), energy dispersive spectroscopy (EDS) (Link-Isis) and X-ray diffraction (XRD) (Rigakumsg-158) techniques. The lamellar spacing was statistically measured by scanning the cross-sectional images along a chosen line being perpendicular to most of the phase domains traversed, and then calculating the number of identical pixels in successive segments along the line [7, 16–18]. The lamellar spacings were measured by repeating at least 400–500 times. The average lamellar spacing is calculated by the arithmetic average of all the measured values.

The mechanical properties (hardness and fracture toughness) are examined on the polished surface by using the Vickers indentation technique following the ASTM C1327-99 standard. The indentations were made using 9.8 N loads for 15 s, and at least 10 valid microindentations were conducted in each sample. The hardness and fracture toughness are calculated according to the following equations proposed by Niihara [19] for Palmqvist cracks:

$$Hv = 1.8544 \cdot P/a^2 \tag{1}$$

$$K_{IC} = 0.016 \cdot (E_C/Hv)^{2/5}\left(P/al^{1/2}\right) \tag{2}$$

where Hv is the Vickers hardness, K_{IC} the fracture toughness, E_C the elastic modulus of the ceramic, P the indentation load, a half the indentation diagonal and l the crack length [20–22].

Result and discussion

Microstructure evolution

The Al_2O_3/YAG/ZrO_2 ternary hypereutectic samples are approximately 4 mm in diameter. Pore-free samples with smooth surface were obtained in lower scanning rate (<200 μm/s).

Figures 2 and 3 show the EDS spectra of the component phases and the XRD pattern for the ternary hypereutectic, respectively. The relevant analyses indicate that the Al_2O_3/YAG/ZrO_2 hypereutectic consists of Al_2O_3 phase, YAG phase and ZrO_2 phase, which are black, gray and white in SEM photography, respectively. The volume fraction of different composition phases is given in Table 1. With lower scanning rate, the microstructure exhibits weakly irregular property due to unidirectional heat flow and branching of facet phase (see Figure 4(a)). The ZrO_2 phase is observed mainly as lamellar

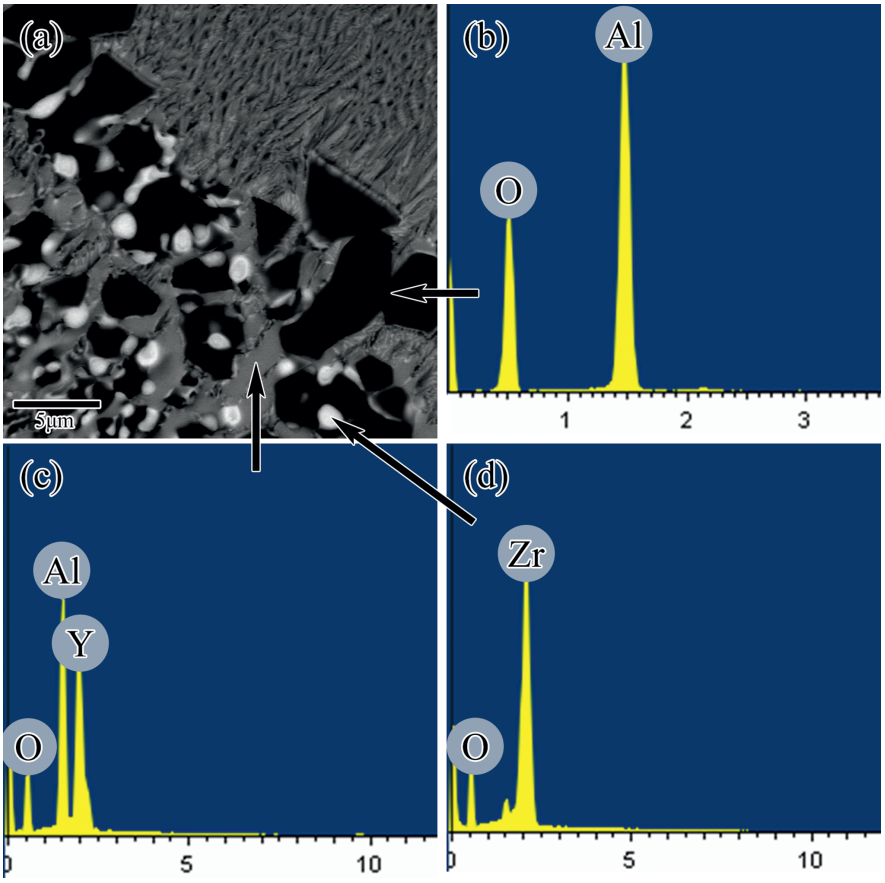

Figure 2: The microstructure of the as-solidified hypereutectic sample (a) and the corresponding EDS analysis of the alumina (b), YAG (c) and zirconia (d).

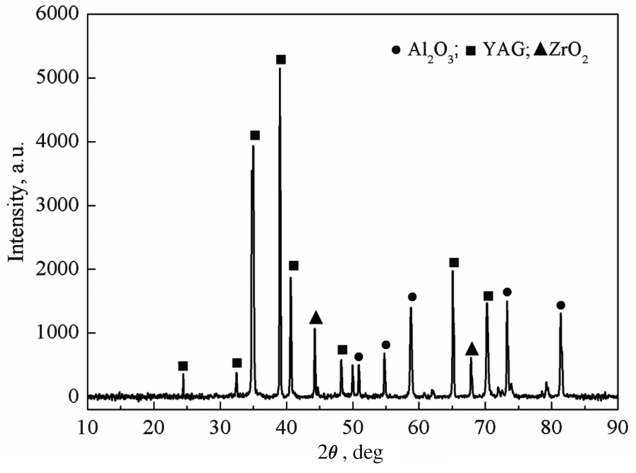

Figure 3: XRD pattern of the as-solidified Al_2O_3/YAG/ZrO_2 ternary hypereutectic.

morphology between Al_2O_3 and YAG. In higher solidification velocity, the microstructure is refined obviously and transforms to regular lamellar morphology. It is found that the lamellar spacing remains almost as constant at very high solidification velocity (see Figure 4(d)). The

Table 1: Elastic modulus, linear thermal expansion coefficient and volume fraction of different composition phases.

Composition phase	Elastic modulus (E, GPa)	Linear thermal expansion coefficient ($K^{-1} \times 10^{-6}$)	Volume fraction (f, %)
Al_2O_3	390	8.4	39.25
YAG	310	8.0	42.25
ZrO_2	220	12.65	18.5

Source: Data from Refs [34–36].

ZrO_2 phase is hardly observed in SEM at very high solidification velocity that is similar to other reports [12].

Compared with Al_2O_3/YAG/ZrO_2 eutectic prepared under same solidification condition [12], the hypereutectic microstructure exhibits obvious texturing tendency. The eutectic microstructure is mainly composed of interconnected Al_2O_3 and YAG (so-called Chinese script), and the ZrO_2 phase partially distributes between Al_2O_3/YAG interfaces or at the edge of the YAG phases [9]. The

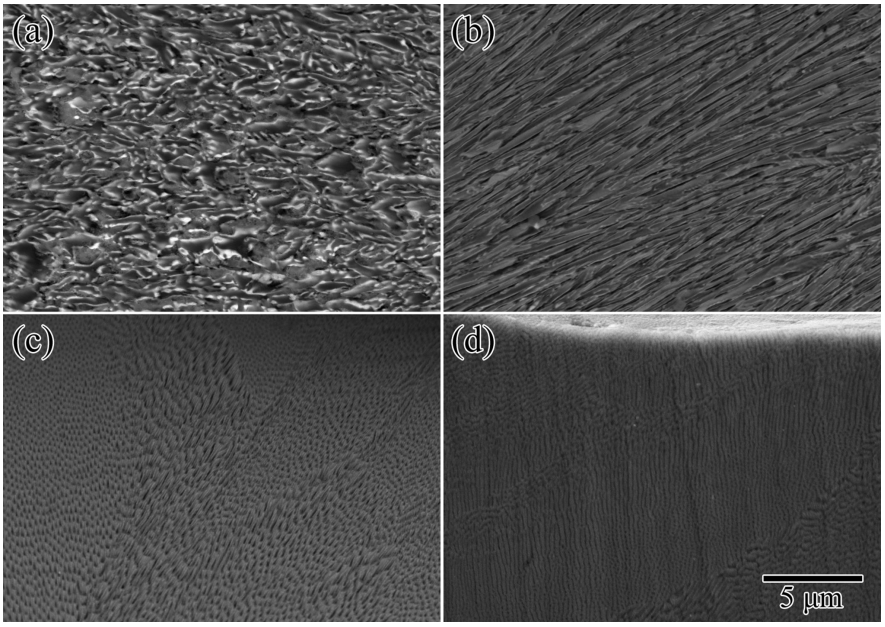

Figure 4: Microstructures of Al_2O_3/YAG/ZrO_2 hypereutectic with different solidification velocities: (a) 100 μm/s; (b) 200 μm/s; (c) 400 μm/s; (d) 800 μm/s.

growth characteristic of hypereutectic exhibits intensely texturing tendency, which is similar with the regular eutectic.

The texturing tendency of hypereutectic microstructure is the result of the ZrO_2 addition. In Al_2O_3/YAG binary system, the irregular morphology is caused by the strong anisotropy of Al_2O_3 [23]. However, the microstructure of Al_2O_3/YAG/ZrO_2 is mainly controlled by YAG and ZrO_2 phases. As shown by the solid/liquid interface of Al_2O_3/YAG/ZrO_2 hypereutectic [24], the YAG phase projects into the melt [15]. And in the Al_2O_3/YAG/ZrO_2 ternary system, YAG and ZrO_2 dissolve each other. However, Al_2O_3 solubility in solid solutions YAG and ZrO_2 is almost zero [25, 26]. So YAG and ZrO_2 easily form lamellar microstructure with more coincident spacing through diffusion couple. Thus, in coupled growth of Al_2O_3/YAG/ZrO_2 ternary hypereutectic, the microstructure is governed by YAG and ZrO_2, which are leading phases with regular lamellar spacing.

Furthermore, the very high-temperature gradient and solidification velocity supplied by horizontal laser zone melting method are also important reasons for texturing tendency of microstructure. The samples obtained by the conventional method with a lower temperature gradient (i. e. Bridgman method [1], 10^2 K/cm) have "Chinese script" microstructure. However, the microstructure obtained with a higher temperature gradient, such as laser floating zone (LFZ) method (6×10^3 K/cm) [12] and μ-PD method (10^3 K/cm) [7], has more regular microstructure. The morphology of the irregular eutectic is determined by the branching of the faceted phase. The higher temperature gradient prompts the solid/liquid interface of the faceted phase to be flatter, which induces the branching of the faceted phase more different and results in the texturing tendency of microstructure. Moreover, with an increase of solidification rate, the texturing tendency is further enhanced. As shown in Figure 4(d), when the solidification rate is 800 μm/s, the microstructure is composed of clusters with regular lamellar whose spacing is almost a constant. Under the rapid solidification condition, the weakly faceted phase or faceted phase may transit into the non-faceted phase [27], which induces a relevant regular eutectic structure [28]. Additionally, the $\lambda v^{0.5} = C$ law (JH model [29]) is universally followed by eutectic growth, where λ is the lamellar spacing, v is the solidification velocity and C is a constant. For the Al_2O_3/YAG/ZrO_2 hypereutectic prepared by the horizontal laser zone melting, C is equal to $7\,\mu m^{1.5} \cdot s^{-0.5}$, lower than that measured from the laser floating zone method [30].

Hardness and fracture toughness

The measured hardness with the different solidification velocity is plotted in Figure 5(a). The maximum hardness of Al_2O_3/YAG/ZrO_2 hypereutectic is 15.9 GPa, slightly larger than that reported on Al_2O_3/YAG/ZrO_2 eutectic fiber prepared by LFZ method (14.8 GPa) [12] and lower than that prepared by optical floating zone method (19.8 GPa) [13]. As shown in Figure 5, the average hardness of Al_2O_3/YAG/ZrO_2 hypereutectic is slightly lower than that of the eutectic.

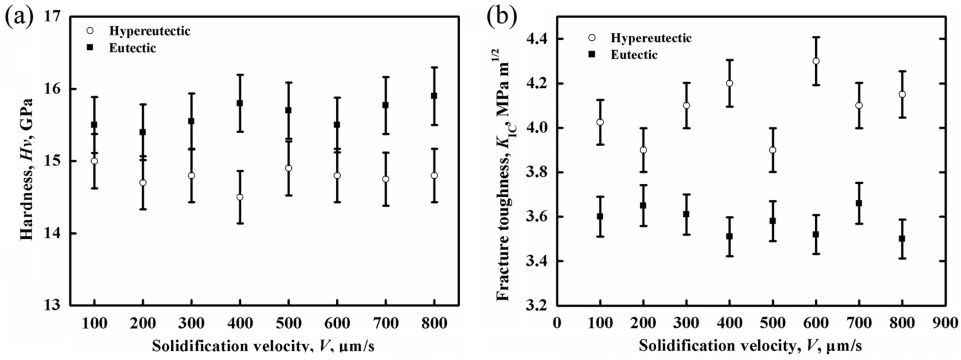

Figure 5: The dependence of the hardness (a) and fracture toughness (b) of Al_2O_3/YAG/ZrO_2 hypereutectic and eutectic in situ composite as a function of the solidification velocity.

In this paper, the elastic modulus of composites (E_C) was calculated by Halpin–Tsai equation [31]:

$$E_C = E_{Al_2O_3} f_{Al_2O_3} + E_{YAG} f_{YAG} + E_{ZrO_2} f_{ZrO_2} \quad (3)$$

The elastic modulus (E) and volume fraction (f) of composition phases are shown in Table 1. The calculated elastic modulus of Al_2O_3/YAG/ZrO_2 hypereutectic is 324.75 GPa. Further, the fracture toughness is also plotted in Figure 5(b). It can be found that the fracture toughness of Al_2O_3/YAG/ZrO_2 hypereutectic is obviously higher than that of eutectic. The maximum of the fracture toughness is 4.2 MPa · m$^{1/2}$. Additionally, the fracture toughness in this work is obviously higher than that obtained from Al_2O_3/YAG eutectic manufactured by the analogous method (2 MPa · m$^{1/2}$) [10]. It illustrates that ZrO_2 plays a role on toughening the Al_2O_3-based in situ composite.

It is widely recognized that the toughening effect of ZrO_2 arises from the discrepancy in the thermal expansion coefficients of the ZrO_2, YAG and Al_2O_3 phases as shown in Table 1. Because Al_2O_3 and YAG phases have similar thermal expansion coefficients, the residual stresses are almost free in Al_2O_3/YAG binary eutectic. However, the thermal expansion coefficient of ZrO_2 is much higher than those of YAG and Al_2O_3. Therefore, ZrO_2 is subjected to tensile residual stresses. Al_2O_3 and YAG phases are often subjected to compressive residual stresses in the Al_2O_3/YAG/ZrO_2 ternary system [32, 33]. According to Frazer [33], the residual tensile stress in ZrO_2 reaches 1.13 GPa in Al_2O_3/YAG/ZrO_2 ternary system. The interaction between the high residual stresses and the propagating cracks is the direct reason for the toughening effect [24]. Additionally, the improved fracture toughness can be attributed to the microstructure with obviously regular eutectic characteristic. The relevant results reported by Song et al. [24] illustrate that the crack propagation can be significantly affected by the phase interface in Al_2O_3/YAG/ZrO_2 eutectic system. The propagating cracks can be disturbed more easily by the intense and regularly arranged phase interface.

Conclusion

Hypereutectic Al_2O_3/YAG/ZrO_2 in situ composite is prepared by the horizontal laser zone melting technique. With the increase of solidification velocity, the microstructure transits from weakly regular to regular lamellar eutectic. The regular eutectic microstructure with almost constant lamellar spacing is obtained under solidification velocity of 800 μm/s. Compared with Al_2O_3/YAG/ZrO_2 ternary eutectic obtained under same solidification condition, the hypereutectic microstructure exhibits obvious texturing tendency. This is mainly due to the addition of ZrO_2 which projects into the melt with YAG together. The two phases form regular eutectic, which plays the leading role in the eutectic solidification and results in the relatively regular eutectic morphology. Furthermore, the very high-temperature gradient and solidification velocity supplied by horizontal laser zone melting method are also important reasons for texturing tendency. The maximum hardness and fracture toughness are 15.9 GPa and 4.2 MPa · m$^{1/2}$, respectively.

Funding: Thanks are given to the National Natural Science Foundation of China (grant/award no. 51501154, 51323008, 51105311 and 51271213), National Basic Research Program of China (grant/award no. 2011CB610402), National High Technology Research and Development Program of China (grant/award no. 2013AA031103), China Postdoctoral Science Foundation (grant/award no. 2015M572597) and Specialized Research Fund for the Doctoral Program of Higher Education of China (grant/award no. 20116102110016).

References

[1] Y. Waku, N. Nakagawa, T. Wakamoto, H. Ohtsubo, K. Shimizu and Y. Kohtoku, Nature, 389 (1997) 49–52.

[2] Y. Waku, N. Nakagawa, T. Wakamoto, H. Ohtsubo, K. Shimizu and Y. Kohtoku, J. Mater. Sci., 33 (1998) 1217–1225.

[3] Y. Waku, N. Nakagawa, T. Wakamoto, H. Ohtsubo, K. Shimizu and Y. Kohtoku, J. Mater. Sci., 33 (1998) 4943–4951.

[4] M. Fritsch and H. Klemm, J. Eur. Ceram. Soc., 28 (2008) 2353–2358.

[5] M. Fritsch, H. Klemm, M. Herrmann and B. Schenk, J. Eur. Ceram. Soc., 26 (2006) 3557–3565.

[6] S. Ochiai, T. Ueda, K. Sato, M. Hojo, Y. Waku, N. Nakagawa, S. Sakata, A. Mitani and T. Takahashi, Compos. Sci. Technol., 61 (2001) 2117–2128.

[7] J.H. Lee, A. Yoshikawa, T. Fukuda and Y. Waku, J. Cryst. Growth, 231 (2001) 115–120.

[8] B.M. Epelbaum, A. Yoshikawa, K. Shimamura, T. Fukuda, K. Suzuki and Y. Waku, J. Cryst. Growth, 198–199 (1999) 471–475.

[9] A. Larrea, V.M. Orera, R.I. Merino and J.I. Peña, J. Eur. Ceram. Soc., 25 (2005) 1419–1429.

[10] J.Y. Pastor, J. LLorca, A. Salazar, P.B. Oliete, I. DeFrancisco and J.I. Peña, J. Am. Ceram. Soc., 88 (2005) 1488–1495.

[11] J.M. Calderon-Moreno and M. Yoshimura, J. Eur. Ceram. Soc., 25 (2005) 1365–1368.

[12] J.I. Peña, M. Larsson, R.I. Merino, I.D. Francisco, V.M. Orera, J. LLorca, J.Y. Pastor, A. Martín and J. Segurado, J. Eur. Ceram. Soc., 26 (2006) 3113–3121.

[13] L. Mazerolles, N. Piquet, M. Trichet, L. Perrière, D. Boivin and M. Parlier, Aerosp. Sci. Technol., 12 (2008) 499–505.

[14] P.B. Oliete, J.I. Peña, A. Larrea, V.M. Orera, J. LLorca, J.Y. Pastor, A. Martín and J. Segurado, Adv. Mater., 19 (2007) 2313–2318.

[15] K. Song, J. Zhang, X. Jia, H. Su, L. Liu and H. Fu, J. Eur. Ceram. Soc., 33 (2013) 1123–1128.

[16] J.H. Lee, A. Yoshikawa, S.D. Durbin, D. Ho Yoon, T. Fukuda and Y. Waku, J. Cryst. Growth, 222 (2001) 791–796.

[17] A. Yoshikawa, B.M. Epelbaum, K. Hasegawa, S.D. Durbin and T. Fukuda, J. Cryst. Growth, 205 (1999) 305–316.

[18] K. Song, J. Zhang, X. Jia, H. Su, L. Liu and H. Fu, J. Cryst. Growth, 345 (2012) 51–55.

[19] K. Niihara, J. Mater. Sci. Lett., 2 (1983) 221–223.

[20] B. Ballóková, M. Besterci and P. Hvizdoš, High Temp. Mat. Pr.-Isr., 34 (2015) 317–323.

[21] R.D. Bedse, J.K. Sonber, K. Sairam, T.S.R.C. Murthy and R.C. Hubli, High Temp. Mat. Pr.-Isr., ISSN (Online) 2191–0324, ISSN (Print) 0334–6455, DOI: 10.1515/htmp-2014-0084 (January 2015).

[22] S. Adamiak, W. Bochnowski, A. Dziedzic, R. Filip and E. Szeregij, High Temp. Mat. Pr.-Isr., ISSN (Online) 2191–0324, ISSN (Print) 0334–6455, DOI: 10.1515/htmp-2014-0139 (February 2015).

[23] Y. Mizutani, H. Yasuda, I. Ohnaka, N. Maeda and Y. Waku, J. Cryst. Growth, 244 (2002) 384–392.

[24] K. Song, J. Zhang, X. Lin, L. Liu and W. Huang, J. Eur. Ceram. Soc., 34 (2014) 3051–3059.

[25] S.M. Lakiza and L.M. Lopato, J. Am. Ceram. Soc., 80 (1997) 893–902.

[26] J.M. Calderon-Moreno and M. Yoshimura, Mater. Sci. Eng. A, 375–377 (2004) 1250–1254.

[27] Z. Jian, K. Kuribayashi and W. Jie, Acta Mater., 52 (2004) 3323–3333.

[28] K. Song, J. Zhang and L. Liu, Scripta Mater., 92 (2014) 39–42.

[29] K.A. Jackson and J.D. Hunt, Trans. Metall. Soc. AIME, 236 (1966) 1129–1142.

[30] K. Song, J. Zhang, X. Jia, H. Su, L. Liu and H. Fu, Acta Metall. Sin., 48 (2012) 220–226.

[31] S.W. Tsai and H.T. Hahn, Introduction to Composite Materials, Technomic. Pub. Co, Lancaster (1980).

[32] J. LLorca and V.M. Orera, Prog. Mater. Sci., 51 (2006) 711–809.

[33] C.S. Frazer, Thermal residual stresses in directionally-solidified Alumina-YAG and Alumina-Zirconia eutectic composites: measurement and modeling [PhD thesis], Elizabeth Dickey (MI), University of Kentucky (2003).

[34] V.M. Orera, R. Cemborain, R.I. Merino, J.I. Peña and A. Larrea, Acta Mater., 18 (2002) 4677–4686.

[35] W.J. Alton and A.J. Barlow, J. Appl. Phys., 38 (1967) 3023–3024.

[36] J.A. Pardo, R.I. Merino, V.M. Orera, J.I. Peña, C. González, J.Y. Pastor and J. LLorca, J. Am. Ceram. Soc., 11 (2000) 2745–2752.